CHAPTER III

IN VITRO BIOCOMPATIBILITY OF ELECTROSPUN AND SOLVENT-CAST CHITOSAN SUBSTRATA TOWARDS SCHWANN, OSTEOBLAST, KERATINOCYTE AND FIBROBLAST CELLS

3.1 ABSTRACT

Chitosan or poly(N-acetyl-D-glucosamine-co-D-glucosamine) with a degree of deacetylation of about 85% was fabricated into nanofibrous membranes by electrospinning from 7% w/v chitosan solution in 70:30 v/v trifluoroacetic acid/dichloromethane solvent system. The obtained fibers were smooth without the presence of beads. The diameters of the individual fiber segments were 126 ± 20 nm. The potential for use of the electrospun chitosan nanofibrous membranes as substrates for cell/tissue culture was evaluated with four different cell types, i.e., schwann cells, osteoblast-like cells, keratinocytes and fibroblasts, in terms of the attachment and the proliferation of the cells as well as the morphology of the seeded and the cultured cells. The results were compared with the corresponding solvent-cast films. Both types of the chitosan substrates supported the attachment and, at the same time, promoted the largest increase in the viability of the cultured keratinocytes. The viability of schwann cells cultured on these substrates increased marginally well, but the attachment of the cells on the surfaces was relatively poor. Finally, both types of the chitosan substrates showed cytostatic property towards both osteoblast-like cells and fibroblasts, despite the convincingly good attachment of osteoblast-like cells on the surfaces.

(**Keywords**: Electrospinning; Fibrous membranes; Chitasan; Biocompatibility)

3.2 Introduction

Tissue engineering is an interdisciplinary technology that applies materials engineering, cellular biology and genetic engineering towards the development of biological substitutes for tissues, such as skin, cartilage for joints, bone and so on [1]. The primary objectives of these substitutes are to restore, maintain and/or improve tissue functions. A functional scaffold for tissue engineering must support and define the three-dimensional (3D) organization of the tissue-engineered space and maintain the normal differentiated state of cells within the cellular compartment. Ideally, a functional scaffold should mimic the structure and biological function of native extracellular matrix (ECM) proteins [2], so as to provide mechanical support and regulate cellular activities [3]. A wide variety of fabrication techniques have been used to generate 3D polymeric scaffolds for potential use in tissue regeneration. Electrospinning is a technique capable of producing ultra-fine fibers with diameters in sub-micrometer down to nanometer range through the action of a high electric field [4]. Under such a high electric field, a stream of a polymer liquid (solution or melt) is ejected towards a collector. It undergoes a significant stretching while the solvent being evaporated, resulting in the deposition of solid fibers in the form of a non-woven fabric on the collector [4]. The 3D structure and topography of the electrospun polymeric fiber mats resemble those of the collagen bundles in the natural ECM [2]. Other characteristics, such as high surface area, high porosity and high inter-pore connectivity, make electrospun fiber mats excellent candidates for tissue engineering [2, 3, 5-7].

Over the past decade, development of scaffolds for cell/tissue culture based on biodegradable and biocompatible synthetic or natural polymers has been investigated [8-12]. Among the various natural polymers, chitosan has been widely explored as a suitable functional material for biomedical applications, due mainly to its biocompatibility, biodegradability and non-toxicity [13]. Chitosan or poly(*N*-acetyl-D-glucosamine-*co*-D-glucosamine) is a partially *N*-deacetylated derivative of chitin or poly(*N*-acetyl-D-glucosamine), one of the most abundant polysaccharides, derived predominantly from shells of arthropods as well as internal flexible backbone of cephalopods [13]. Direct electrospinning of chitosan has proven to be quite

problematic [14]. Consequently, electrospinning of chitosan has usually been carried out from its blend solutions with another electrospinnable polymer, such as poly(ethylene oxide) (PEO) in an aqueous solution of acetic acid [15-17], or acetic acid, hydrochloric acid, or trifluoroacetic acid (TFA) [18]; ultra-high molecular weight PEO in a mixture of an aqueous solution of acetic acid and dimethyl sulfoxide [19]; silk fibroin in an aqueous solution of formic acid [20]; poly(vinyl alcohol) (PVA) in an aqueous solution of formic acid [14], acetic acid [14, 21-26], or acrylic acid [27-29]; PVA and poly(vinyl pyrrolidone) (PVP) in an aqueous solution of acetic acid [30]; poly(ethylene terephthalate) (PET) in TFA [31]; type I collagen in a mixed solvent system of 1,1,1,3,3,3-hexafluoro-2-propanol (HFP) and TFA [32-34]; type I collagen and PEO in an aqueous solution of acetic acid [35]; polyacrylamide (PAAm) in an aqueous solution of acetic acid [36]; poly(lactic acid) (PLA) in TFA [37]. Also, electrospinning of chitin or chitosan derivatives and its blend polymer solutions has been reported, such as carboxymethyl chitin [38], carboxyethyl chitosan [39] with poly(vinyl alcohol) in distilled water; hexanoyl chitosan in chloroform [40]; quaternized chitosan derivative with poly(vinyl pyrolidone) [41], or poly(vinyl alcohol) [42] in an aqueous solution.

Notwithstanding, successful fabrication of pure chitosan nanofibers has been reported from the electrospinning of chitosan solutions in TFA or a mixture of TFA and dichloromethane (DCM) [14, 31, 43-51], deacetylation of chitin nanofibers obtained from the electrospinning of chitin solutions in HFP [52], and the electrospinning of chitosan solutions in 90% aqueous acetic acid solution [54, 54]. Pure chitosan nanofibers could also be obtained by a two-step approach: the preparation of bicomponent nanofibers of chitosan and another electrospinnable polymer (e.g., PVA) and the subsequent removal of the polymer by solvent-extraction [21, 25]. Coaxial electrospinning, with chitosan forming the core and PEO forming the sheath, can alternatively be used to prepare pure chitosan nanofibers by subsequent removal of the PEO sheath [55]. Based on these previous reports [14, 31, 43-51], the use of TFA, with or without DCM as the modifying co-solvent, as the solvent system for the fabrication of pure chitosan nanofibers by electrospinning has been shown to be most effective. However, further utilization of the chitosan nanofibrous membranes that are prepared from chitosan solutions in TFA or

TFA/DCM is often limited by the loss of the fibrous structure as soon as the membranes are in contact with an aqueous medium [43, 46, 47]. The dissolution of the electrospun chitosan fibers from the chitosan solutions in TFA or TFA/DCM occurs as a result of the high solubility in the aqueous medium of the $-NH_3^+CF3COO^-$ salt residues that are formed when chitosan is dissolved in TFA [43]. The dissolution of the chitosan nanofibrous membranes in an aqueous medium can be alleviated by cross-linking with glutaraldehyde [46, 47]. The use of glutaraldehyde as the cross-linking agent via either the one- [47] or the two-step [46] cross-linking process rendered the cross-linked fibers to be swellable, but insoluble, in neutral and acidic aqueous media. However, the biodegradability of the cross-linked chitosan fibers may be adversely affected, if the extent of cross-linking is too great.

In a previous work [43], the stabilization of the chitosan nanofibrous membranes in an aqueous medium could be achieved by immersing the membranes in 5 M Na_2CO_3 aqueous solution for 3 h at ambient condition. It was shown that the post-neutralized membranes could maintain their fibrous structure even after a continuous submersion in phosphate buffer saline (PBS, pH = 7.4) or distilled water for 12 weeks. As an evidence for actual usefulness of the proposed neutralization method, it was shown that the post-neutralized chitosan nanofibrous membranes could be used as substrates for *in vitro* biocompatibility study with a schwannoma cell line, RT4-D6P2T [6]. Recently, Wan et al. [49] utilized the proposed neutralization procedure to ascertain the stability of both the poly(chitosan-*g*-DL-lactic acid) (PCLA) and the chitosan scaffolds prepared by electro-wet-spinning process in the cell culturing condition using primary dermal fibroblasts harvested from a New Zealand rabbit as reference.

Despite the numerous report on the in vitro responses of difference cell lineages on blend and pure electrospun chitosan nanofibers [6, 17, 35, 40, 44], a similar report that study the *in vitro* responses and cellular behavior of any type of the cell lineages on pure chitosan nanofibrous scaffolds is still lacking. Here, we report, the *in vitro* biological evaluation of the pure electrospun chitosan nanofibrous membranes towards four different types of cells, i.e., Schwann cells, osteoblast-like

cells, keratinocytes and fibroblasts, in comparison with the corresponding solvent-cast films and the tissue-culture polystyrene plate (TCPS).

3.3 Experimental details

3.3.1 Materials

Chitosan [powder, degree of deacetylation (%DDA) ~ 85%; see detailed characterization in supplementary data], trifluoroacetic acid (TFA, CF_3COOH; ~98% purity) and dichloromethane (DCM) were purchased from Sigma-Aldrich (USA). Na_2CO_3, used as a neutralizing agent, was purchased from Sigma-Aldrich (USA). Both the weight-average and the number-average molecular weights of chitosan were determined to be about 610 and 110 $kg \cdot mol^{-1}$, respectively (see detailed characterization in supplementary data).

3.3.2 Fabrication of Electrospun Chitosan Nanofibrous Membranes and Corresponding Solvent-Cast Films

Electrospun chitosan nanofibrous membranes were prepared in a manner similar to a previous report [43]. Briefly, 7% w/v chitosan solution was prepared by dissolving a measured amount of chitosan powder in 70:30 v/v TFA/DCM mixture. The as-prepared chitosan solution was stirred continuously for 12 h at room temperature and later fed into a 5-mL glass syringe fitted with a blunt 20-gauge stainless steel needle (OD = 0.91 mm), used as the nozzle. Both the syringe and the needle were tilted 45° from a horizontal baseline. The electrospun chitosan nanofibers were collected on an aluminum sheet wrapped around a homemade rotating cylinder (width and diameter ≈ 15 cm; 40-50 rpm), placed at a fixed distance of 20 cm from the needle tip. The needle was connected to the emitting electrode of positive polarity of a Gamma High-Voltage Research ES30P-5W power supply. Both the electrical potential and the collection time were fixed at 25 kV and 24 h. The solution feed rate was driven mainly by the gravity and the electrostatic forces generated during electrospinning. The resulting chitosan nanofibrous membranes were dried *in vacuo* at room temperature prior to further investigation.

To further stabilize the chitosan nanofibrous membranes in the cell culturing medium, the membranes were subjected to neutralization by a method previously proposed by some of us [43]. Briefly, the membranes were immersed in 5 M Na_2CO_3 aqueous solution for 3 h at ambient condition. After the immersion, the membranes were repeatedly washed with distilled water until of neutral pH, dried at ambient condition for 1 d and further dried in an oven at 40 °C overnight prior to further studies.

For comparison purposes, chitosan was also fabricated into films by the solution-casting technique. The casting chitosan solution (at 2.5% w/v) was prepared by dissolving a measured amount of chitosan powder in 1 wt.% acetic acid aqueous solution. After having been stirred until a clear solution was obtained, it was cast on glass Petri dishes and dried *in vacuo* at room temperature prior to further investigation.

3.3.3 Wettability of Electrospun Chitosan Nanofibrous Membranes and Corresponding Solvent-Cast Films

Wettability of the chitosan nanofibrous membranes and the corresponding film surfaces was assessed by water contact angle measurements. The static water contact angles were measured by a sessile drop method using a Krüss contact angle measurement system. A distilled water droplet (about 40 μL) was gently plated on the surface of each specimen. At least 10 readings on different parts of the specimen were averaged to attain a data point.

3.3.4 Cell Culture and Cell Seeding

To evaluate the potential for use of the electrospun chitosan nanofibrous membranes as scaffolding materials, their biocompatibility in terms of cell attachment and cell proliferation towards four different cell lineages, including murine Schwann cells (RT4-D6P2T; a schwannoma cell line derived from a *N*-ethyl-*N*-nitrosourea (ENU)-induced rat peripheral neurotumor), murine osteoblast-like cells (MC3T3-E1; mouse calvaria-derived, preosteoblastic cells), human keratinocytes (HaCaT; an immortalized, but non-tumorigenic cell line) and human foreskin fibroblasts (HFF; a non-transformed cell line, originating from pooled foreskins of children), was evaluated in comparison with that of the corresponding films and TCPS.

RT4-D6P2T and MC3T3-E1 were first cultured as a monolayer in Dulbecco's modified Eagle's medium (DMEM; Sigma-Aldrich, USA), supplemented by 5% fetal bovine serum (FBS; Biochrom AG, Germany), 1% L-glutamine (Invitrogen, USA) and 1% antibiotic and antimycotic formulation [containing penicillin G sodium, streptomycin sulfate and amphotericin B (Invitrogen, USA)]. The cells were incubated at 37 °C in a humidified atmosphere containing 5% CO_2 and the culture medium was replaced once in every 2 d. Each of the free-standing chitosan nanofibrous membranes (see Figure 3.1) and the film specimens was cut into circular disks (~15 mm in diameter) and the disk specimens were placed in wells of a 24-well tissue-culture polystyrene plate (TCPS; Biokom System, Poland), which were later sterilized in 70% ethanol for 30 min. The specimens were then washed with autoclaved deionized water and subsequently immersed in DMEM overnight. To ensure a complete contact between the specimens and the wells, each specimen and also TCPS was pressed with a stainless steel ring (stainless steel grade 304; ~14 mm in diameter). The reference cells from the cultures were trypsinized [0.25% trypsin containing 1 mM ethylenediaminetetraacetic acid (EDTA; Invitrogen, USA)], counted by a haemocytometer (Hausser Scientific, USA) and seeded at a density of about 40,000 cells/well on both the fiber mat and the film specimens and empty wells of TCPS that were used as control.

HaCaT and HFF were also cultured based on the same procedure but slightly different in the ingredients of the cell culturing medium supplement, i.e., 10% fetal bovine serum (FBS, BIOCHROM, Germany), 1% L-glutamine (Invitrogen, USA), together with 100 units·mL^{-1} penicillin (Invitrogen, USA) and 100 μg·mL^{-1} streptomycin (Invitrogen, USA).

3.3.5 Cell Attachment and Cell Proliferation

For the cell attachment study, the reference cells were seeded on both the nanofiber mat and the film specimens in wells of a 24-well TCPS at 40,000 cells/well and allowed to attach to the surfaces of the specimens for 2, 8 and 24 h. The viability of the cells in bare wells of the TCPS was used as control. At each specified seeding time, the viability of the attached cells was quantified by 3-(4,5-dimethylthiazol-2-yl)-2,5-diphenyl-tetrazolium bromide (MTT) assay. Each

specimen was rinsed with phosphate-buffered saline (PBS; Sigma-Aldrich) to remove unattached cells prior to the MTT assay. For the cell proliferation study, the cells were first seeded on both the nanofiber mat and the film specimens in wells of a 24-well TCPS at 40,000 cells/well and a priori allowed to attach to the specimens for 24 h. The viability of the proliferated cells on the specimens was quantified by the MTT assay after the cells had been cultured for 1, 3 and 5 d. The method was similar to the cell attachment study except for the fact that the culture medium was replaced with SFM on days 1 and 3 in order to get rid of the effect of the nutrients that are present in the medium on the increase in the viability of the cultured cells.

3.3.6 Quantification of Viable Cells by MTT Assay

The MTT assay is the method used to quantify the viability of cells on the basis of the reduction of the yellow tetrazolium salt to purple formazan crystals by dehydrogenase enzymes secreted from the mitochondria of metabolically active cells. The amount of purple formazan crystals relates to the number of the viable cells in a linear manner. First, the culture medium of each cultured specimen was removed and replaced with 500 μL/well of MTT solution (Sigma-Aldrich, USA) and then the plate was incubated for 1 h. After incubation, the MTT solution was removed. Then, 500 μL/well of dimethyl sulfoxide (DMSO; Riedel-de Haën, Germany) was added to dissolve the formazan crystals and the plate was left at room temperature in darkness for 1 h on a rotary shaker. Finally, the absorbance at 570 nm, representing the proportion of the viable cells, was recorded by a Thermospectronic Genesis10 UV-visible spectrophotometer.

3.3.7 Statistical Analysis

The data are presented as means ± standard errors of the means (n = 3). A one-way ANOVA was used to compare the means of different data sets and a statistical significance was accepted at a 0.05 confidence level.

3.3.8 Morphological Observation of Cultured Cells

After the culture medium had been removed, the cell-cultured fiber mat and film specimens were rinsed with PBS twice and the cells were fixed with 3% glutaraldehyde solution [diluted from 50% glutaraldehyde solution (Electron Microscopy Science, USA) with PBS] at 500 μL/well. After 30 min, they were

rinsed again with PBS and kept in PBS at 4 °C. After cell fixation, the specimens were dehydrated in an ethanol solution of varying concentration (i.e., 30, 50, 70 and 90%) and, finally, with pure ethanol for about 2 min each. The specimens were then dried in 100% hexamethyldisilazane (HMDS; Sigma-Aldrich, USA) for 5 min and later dried in air after the removal of HMDS. After being completely dried, the specimens were mounted on copper stubs, coated with gold using a JEOL JFC-1100E sputtering device for 3 min and observed by a JEOL JSM-5200 scanning electron microscope. For comparison, the morphology of the cells that had been seeded or cultured on a glass substrate (cover glass slide, 1 mm in diameter; Menzel, Germany) was also investigated.

3.4 Results and Discussion

As mentioned, an attempt to mimic the structure and function of the natural ECM has been the most important point for the development of a functional scaffold that can restore, maintain and/or improve the function of tissues. This can be achieved with the right choices of the materials and the methods with which the materials are fabricated. Chitosan, due to the presence of the *N*-acetyl-D-glucosamine co-monomeric unit, is, at least partly, structurally similar to hyaluronic acid or poly(D-glucuronic acid-*co*-*N*-acetyl-D-glucosamine), one of the major glycosaminoglycans (GAGs) of the natural ECM in native tissues [56]. The fabrication of chitosan into fibrous form by electrospinning, with size equivalent to that of the collagen bundles found in the native tissues [2], could render the material a suitable candidate as a functional scaffold for cell/tissue culture.

Here, electrospinning of chitosan was carried out in a manner similar to a previous report [43]. Smooth fibers without the presence of beads were obtained and the diameters of these fibers were 126 ± 20 nm. After consecutive spinning for ~2 d, the thickness of the chitosan nanofibrous membranes was 35 ± 2 μm. As shown in supplementary data, predominantly smooth fibers were only obtained from 7 and 8% w/v chitosan solutions in TFA/DCM, while a combination of smooth and beaded fibers were obtained from 5 and 6% w/v chitosan solutions. While the

electrospinning of chitosan from its solution in TFA was achieved at a low concentration (i.e., 2.7% w/v) [46, 47], the electrospinning of the polymer from its solutions in TFA/DCM, on the other hand, was successfully performed at relatively greater concentrations [14, 43, 45, 48, 50, 51] (see summary of the data obtained from the literature in supplementary data). This could be a result of the reduction in the viscosity of the chitosan solutions due to the presence of DCM as the modifying co-solvent.

In the present work, the potential for use of the electrospun chitosan nanofibrous membranes as substrates for cell/tissue culture was evaluated with four different types of cells, e.g., murine Schwann cells (RT4-D6P2T; hereafter, Schwann cells), murine osteoblast-like cells (MC3T3-E1; hereafter, osteoblast-like cells), human keratinocytes (HaCaT; hereafter keratinocytes) and human fibroblasts (HFF; hereafter, fibroblasts), in terms of the attachment and the proliferation of the cells as well as the morphology of the seeded and the cultured cells. The corresponding solvent-cast films and TCPS were used as the internal and the positive controls, respectively. The thickness of the solvent-cast chitosan films was 72 ± 5 μm. The reason for the aqueous solution of acetic acid being used instead of the TFA/DCM mixture as the casting solvent for the fabrication of chitosan films was due mainly to the cost of TFA. The choice of either solvent system, however, did not have a noticeable effect on the surface morphology of the obtained films (see additional experiment in supplementary data).

It is a known fact that wettability of the surface of a scaffold plays an important role for the adhesion of ECM biomolecules which promote seeded or cultured cells to attach, proliferate and differentiate. Based on a static water contact angle assessment of the surfaces of the electrospun chitosan nanofibrous membranes and corresponding solvent-cast films, it indicated that the wettability of the membrane surfaces was complete as perfect spreading of water droplets was observed (data not shown).

3.4.1 Cell Attachment and Cell Proliferation

The ability to support the attachment of cells is one of the foremost characteristics of a functional scaffold. To evaluate such a characteristic, the reference cells were seeded on the chitosan nanofibrous substrates for various cell

seeding time intervals. The results were compared with those obtained with the corresponding film substrates and TCPS. Figure 3.1 shows the viability of the four different cell types after the cells had been seeded on the chitosan nanofibrous and the film substrates, in comparison with that on TCPS, for 2, 8 and 24 h. The viability of the cells attached on TCPS at 2 h after cell seeding was used as the reference value to calculate the relative viability of the attached cells shown in the figure. For any given cell type, the viability of the attached cells on these substrates generally increased significantly with an increase in the cell seeding time, with an exception to Schwann cells on the nanofibrous substrates which showed a decrease, and fibroblasts on both the nanofibrous and the film substrates which showed a constancy, in their viability between 8 and 24 h of cell seeding.

At any given cell seeding time point, the viability of the cells attached on TCPS was generally greater than that of the cells attached on both the nanofibrous and the film substrates. However, equivalent values were observed for osteoblast-like cells that had been seeded on the nanofibrous substrates for 2 h, keratinocytes that had been seeded on the film substrates for 8 h, and keratinocytes that had been seeded on both the fibrous and the film substrates for 24 h. Comparatively, between the nanofibrous and the film substrates, the viability of Schwann cells, osteoblast-like cells and keratinocytes that had been seeded on the nanofibrous substrates, in most cases, was greater than that of the cells on the film counterparts, with an exception to fibroblasts that had been seeded for 24 h which showed a comparable value. Additionally, the viability of keratinocytes that had been seeded on the nanofibrous substrates for 2 and 8 h was inferior to that of the cells on the film counterparts. However, at 24 h of cell seeding, the viability of the cells on both types of substrates showed equivalent values.

The ability of the different substrates in promoting the attachment of the cells could be evaluated further by observing the viability of the cells attached on a given type of substrates whether it was either increased or decreased between two adjacent seeding time points. Between 2 and 8 h of cell seeding, the largest increase in the viability of the attached Schwann cells and osteoblast-like cells was observed when they were seeded on TCPS, while that of the attached keratinocytes and fibroblasts was observed when they were seeded on the nanofibrous and the film

substrates, respectively. Interestingly, osteoblast-like cells that had been seeded on the film substrates showed an equivalent increase in the viability of the attached cells to that on TCPS. Between 8 and 24 h of cell seeding, the largest increase in the viability of the attached osteoblast-like cells and fibroblasts was observed when they were seeded on TCPS, while that of the attached keratinocytes and osteoblasts-like cells was observed when they were seeded on the nanofibrous and the film substrates, respectively.

The biocompatibility of the chitosan nanofibrous and the corresponding film substrates was further evaluated in terms of their ability to promote the proliferation of the cells that had been allowed to attach on their surfaces, in comparison with that of TCPS, for 24 h. Figure 3.2 shows the viability of Schwann cells, osteoblast-like cells, keratinocytes and fibroblasts that had been cultured on the various substrates for 1, 3 and 5 d. It should be noted that the viability of the cells that had been allowed to attach on the various substrates for 24 h was taken as the viability of the proliferated cells on day 1 and that the viability of the cells that had been cultured on TCPS on day 1 was used as the reference value to determine the relative viability of the proliferated cells shown in the figure. Similar to the attachment assay, the viability of the cells proliferated on the surfaces of these substrates generally increased with an increase in the cell culturing time. However, fibroblasts that had been cultured on the film substrates showed no increase in their viability between days 1 and 3 of cell culturing. The similar behaviors were also observed on osteoblast-like cells and fibroblasts that had been cultured on the film and the nanofibrous substrates between days 3 and 5 of cell culturing, respectively.

Evidently, the viability of the cells that had been cultured on TCPS, at any given cell culturing time point, was consistently greater than that of the cells on both the nanofibrous and the film substrates, with an exception to that of keratinocytes on both the nanofibrous and the film substrates on day 1 which showed equivalent values to that of TCPS. In most cases, the viability of the cells that had been cultured on the nanofibrous substrates, at any given cell culturing time point, was greater than that of the cells on the film counterparts. An exception to this was for Schwann cells that had been cultured on the film substrates for 3 d which showed a reversed trend. Moreover, no appreciable difference in the viability of keratinocytes

that had been cultured on the nanofibrous and the film substrates at any given cell culturing time point was observed. Between days 1 and 3 of cell culturing, the largest increase in the viability of all types of the proliferated cells was observed when they were grown on TCPS. Between days 3 and 5, a similar observation was obtained, with an exception to keratinocytes which showed the largest increase in the viability when they were grown on both types of film and nanofibrous substrates.

3.4.2 Morphology of Attached and Proliferated Cells

The assessment on the ability of a scaffold to support the attachment and to promote the proliferation of the seeded or the cultured cells should not rely solely on the results obtained by the MTT assay. This is because the method, despite its simplicity, only provides a biological snapshot of the mitochondria's activity that is taken to represent the viability of the cells. Any factor that affects to the mitochondria's activity can also affect the MTT absorbance, despite an equivalent number of cells under investigation. To better assess the ability of a scaffold to support the attachment and to promote the proliferation of the cells, morphological observation of the seeded or the cultured cells can give additional information about the phenotypic nature of the cells, intercellular interaction, and possible interaction between the cells and the substrates onto which they adhere. Tables 3.1-3.4 respectively show representative SEM images of Schwann cells, osteoblast-like cells, keratinocytes and fibroblasts that had been seeded or cultured on the surfaces of the chitosan nanofibrous and the corresponding film substrates as well as that of the glass substrates for 2 h, 8 h, 1 d, 3 d and 5 d. It should be noted that the cell seeding/culturing period of 24 h or 1 d was considered both as the late attachment period and as the early proliferation period.

Studies related to the attachment and the proliferation of Schwann cells on the chitosan nanofibrous and the film substrates stem from the facts that Schwann cells play a crucial role during nerve regeneration through the production of growth factors and the excretion of ECM [57]. Development of a functional bioartificial nerve graft, comprised of a biomaterial pre-seeded with Schwann cells, should be an interesting approach for effective nerve regeneration [58]. According to Table 3.1, even at 2 h after cell seeding, the cells cultured on both the film and the glass substrates appeared in their typical spindle shape with bipolar or multipolar

shape. On the contrary, those cultured on the nanofibrous substrates were still round, suggesting that the cells might not be fully attached on the surface. At 8 h and 1 d after cell seeding and cell culturing, the cells on both the film and the glass substrates extended their cytoplasm in the form of thin and long fibrils, similar to lamellipodia, from the leading edges. On the other hand, those cultured on the nanofibrous substrates, despite an evidence of the cells extending their cytoplasm along the individual fibers, were still round. The cytoplasmic expansion of the cells cultured on the nanofibrous substrates was observed for the first time on day 3 after cell culturing. On day 5 after cell culturing, interconnection of the cultured cells on any type of substrates was discernible.

Chitosan was shown to be an effective substrate that supports the initial attachment and the spreading of osteoblasts [59]. According to Table 3.2, osteoblast-like cells that had been seeded on all types of the substrates were round, with the ones that had been seeded on both the film and the glass substrates exhibiting the evidence of lamellipodia on their surface. The round morphology of the cells indicated that the cells might not yet be fully attached on the surfaces of the substrates. At 8 h after cell seeding, the cells that had been seeded on the glass substrates exhibited an evidence of lamellipodia extending from the edge of the cells, but the morphology of the cells was still round. Similarly, the majority of the cells seeded on the nanofibrous substrates were also round, while those on the film counterparts assumed the spindle shape. On day 1 after cell seeding/culturing, the majority of the cells grown on all types of the substrates were spindle-like. Further increasing the culturing time to 3 and 5 d resulted in the expansion of the cytoplasm of the cells grown on the glass substrates to assume a polygonal shape. On the other hand, while the majority of the cells grown on both the nanofibrous and the film substrates still assumed the spindle morphology, the cells that had been cultured on the nanofibrous substrates expanded relatively better.

Studies related to the attachment and the proliferation of keratinocytes and fibroblasts on the chitosan nanofibrous and the film substrates stem from the fact that chitosan has been heavily explored as a promising material for wound healing [60] and artificial skin applications [61-66], due to its haemostatic and antibacterial properties. According to Table 3, keratinocytes on all types of the substrates after 2

and 8 h of cell seeding were still round. Lamellipodia were, however, observed on the surface of these cells. Interestingly, even at the short attachment time point of 8 h, aggregation of adjacent cells was evident. Clearly, these cells exhibited the characteristic cobblestone morphology after they had been seeded on these substrates for only 8 h. On day 1 after cell seeding/culturing, the cells attached on the glass substrates existed in two populations, i.e., round cells with evidence of lamellipodia and spreaded cells that formed intercellular tight junctions with adjacent cells. In a similar manner, the majority of the cells grown on both types of the chitosan substrates were well-expanded, with the cells forming intercellular tight junctions with adjacent cells. On days 3 and 5 after cell culturing, not only the cultured cells were well-expanded, with the cells forming intercellular tight junctions with adjacent cells, they appeared to grow on top of one another, forming into multilayers of a cellular construct. It should be noted that, after about 3 d of cell culturing, the chitosan substrates were well covered with the cells as well as their secreted matrix.

For potential for uses as wound dressing and skin substitutes, all of the chitosan substrates were further evaluated with fibroblasts. According to Table 3.4, the cells that had been seeded on all types of the substrates for 2 h were round. At 8 h after cell seeding, lamellipodia were observed around the edge of the cells seeded on the films, indicating the beginning of cellular expansion. A similar behavior was observed for the majority of the cells seeded on the glass substrates, however with slightly greater extent of cellular expansion. Evidently, only the cells seeded on the nanofibrous substrates were well-expanded. At the cell culturing times greater than or equal to 1 d, the cells that had been grown on the glass substrates assumed their typical spindle morphology and readily spread over the surface. On days 3 and 5 after cell culturing, interconnection of adjacent cells was evident. A similar result was observed with the cells grown on the nanofibrous substrates. On the film substrates however, both round and spindle-like cells were observed on their surface on day 1 after cell seeding/culturing. More expansion of the cells and the interconnection of adjacent, expanded cells were observed when they had been grown on the film surface for the minimum period of 3 d.

3.5 Further Discussion

Studies related to the *in vitro* biocompatibility of chitosan with mammalian cells have usually been conducted on chitosan in the form of solvent-cast films [58-59, 60, 62-67] with various cell types, e.g., Schwann cells (native cells from sciatic nerve fragments of 1-2 d-old neonatal Sprague–Dawley rats) [58] and (primary rat Schwann cells from sciatic nerve) [54], osteoblast-like cells (MC3T3-E1) [60], fibroblasts (e.g., 3T3 [60], L929 [62], native cells from foreskins of children [63], native cells from specimens of skins from healthy donors [64, 67], and normal adult human dermal fibroblasts (NAHDF) [67]), keratinocytes (e.g., native cells from foreskins of children [63], HaCaT [64], and native cells from specimens of skins from healthy donors [67]), and baby hamster kidney cells (BHK21(C13)) [62]. On the other hand, related studies of chitosan in the form of electrospun nanofibrous membranes are quite limited, with few known reports being on fibroblasts (e.g., human embryo skin fibroblasts (hESFs) [45] and native cells from the back skin of a 60 d-old male New Zealand rabbit [49]). Many of these reports showed that many factors affected the *in vitro* biocompatibility of chitosan, i.e., the degree of deacetylation (%DD) [59, 62-64, 66], molecular weight [64], residual proteins [64], and substrate morphology [i.e., film versus microfibers (15 μm in diameter)] [58]. Substrate morphology was also shown to play a major role in mediating the behavior of the cultured cells [58]. Yuan *et al.* [58] showed that despite the fact that the viability of the native rat Schwann cells after having been cultured on the surface of the chitosan membranes for various cell culturing times, ranging from 1 to 14 d, was greater than that observed on the chitosan macrofibers, the cells migrated more readily onto the stereoframe of the fibers than they did on the surface of the films.

The extracellular matrix (ECM) proteins have the capacity to regulate cell behaviors such as adhesion, spreading, growth, and migration [59]. In a cell culture experiment, the factor affect on protein adsorption cab be explained by surface wettability and surface charge [68, 69]. From the literature, it is well known that cells carry a negative surface charge at physiological pH whose magnitude depends upon the composition of the cell-surface carbohydrate [62, 70]. C. Chatelet *et at.* [63] also showed that the cell adhesion is favored by the smoothness of substrates which

allows a better flat adhesion of the cells. In case of chitosan substrate, the cell adhesion cannot be explained by the surface charge on the chitosan substrates because the amino group in chitosan has a pKa-value of about 6.2–7.0, which makes chitosan basically with no electric charge at the physiological pH-values [71]. Therefore, the difference in cell attachment on any type of cell lineages might be strongly depend on the degree of negative surface charge on cell membranes, protein adsorption on the surface substrate and substrate morphology. In addition, the smoothness of the substrate contributes to allow an easier mobility of the cells necessary for cell proliferation [64]. Therefore, the higher of cell adhesion and cell spreading may be provided more chance on cells came into contact, that cause their mitosis ability was improved and had a stimulating effect on cell proliferation.

In the present work, even though the chitosan nanofibrous substrates were slightly better in supporting the attachment and promoting the proliferation of Schwann cells, the cells grown on the surface of the films developed into their phenotypic morphology much faster than they did on the surface of the nanofibrous substrates, with the formation of thin and long fibrils radiating from the leading edges of the cells being evident only after 8 h after cell seeding. A similar result was observed with the cells grown on the glass substrates. These results suggest that Schwann cells may prefer flat over rough surfaces [6]. Here, the surface of the chitosan nanofibrous membranes was considered rough when the sizes of the pores or other irregularities on the surface of the membranes were much smaller than those of the cells. Notwithstanding, a recent study by Wang *et al.* [51] demonstrated that preferential alignment of the underlying chitosan nanofibrous structures could mediate the alignment of Schwann cells that had been cultured on their surfaces through the contact guidance phenomenon.

Fakhry *et al.* [60] showed that, at 1 h after cell seeding, osteoblasts (MC3T3-E1) adhered much better than fibroblasts (3T3) did on the surfaces of the chitosan-coated glasses. However, at 24 h after cell seeding, the number of the attached fibroblasts increased significantly, with the levels being equivalent to those of the attached osteoblasts. At 1 h after cell seeding, osteoblasts already began to spread, while fibroblasts were still round. At 24 h after cell seeding, a combination of spreaded and round fibroblasts was evident [60]. On the other hand, Chatelet *et al.*

[62] showed that while fibroblasts (native cells from foreskin of children) attached twice more than keratinocytes on the surfaces of chitosan of different degrees of acetylation (%DDA; 3-47%), they could not proliferate on these surfaces. They attributed this phenomenon to the very high adhesion of fibroblasts on these surfaces that could inhibit their growth and exhibited a cytostatic property towards fibroblasts: this is not cytotoxic but inhibits cell proliferation. [63]. Others [62, 64-66], on the other hand, showed that film substrates fabricated from chitosan with a relatively high %DDA (i.e., >90) could support the growth of fibroblasts relatively well. In the present work, both the chitosan nanofibrous and the corresponding film substrates exhibited cytostatic property towards osteoblast-like cells and fibroblasts, as suggested by the relative constancy in the MTT viabilities (see Figure 2b,d) and the relatively low number of cells seen on the SEM images (see Tables 2 and 4). On the other hand, as indicated by both of the MTT and the SEM results, both types of the chitosan substrates supported the attachment and the proliferation of keratinocytes extremely well, but they appeared to support the proliferation of Schwann cells only marginally.

3.6 Conclusion

Electrospun nanofibrous membranes of chitosan or poly(N-acetyl-D-glucosamine-co-D-glucosamine) with the %DD of about 85% and the weight- and the number-average molecular weights of 610 and 110 kg mol_1, respectively, were prepared from 7% w/v chitosan solution in 70:30 v/v TFA/DCM. Smooth fibers with the diameters of the individual fiber segments being 126 ± 20 nm were obtained. The membranes were evaluated for their potential for use as substrates for cell/tissue culture on four different cell lineages, i.e., Schwann cells, osteoblast-like cells, keratinocytes and fibroblasts, against the corresponding solvent-cast films. Both types of the chitosan substrates supported the attachment and the proliferation of keratinocytes very wells. Despite the poor attachment on the substrates, Schwann cells proliferated marginally well on these substrates. Finally, despite the good attachment of osteoblast-like cells, both osteoblast-like cells and fibroblasts were not able to proliferate on these substrates.

3.7 Acknowledgments

This work was supported in part by (1) the Ratchadaphisek Somphot Endowment Fund for Research and Research Unit, Chulalongkorn University and (2) the Center for Petroleum, Petrochemicals and Advanced Materials (CPPAM). P. Sangsanoh thanks a doctoral scholarship (PHD/0191/2550) received from the Royal Golden Jubilee Ph.D. Program, the Thailand Research Fund (TRF).

3.7 References

[1] Langer, R.; Vacanti, J.P. Tissue engineering, *Science* **1993**, 260, 920-926.

[2] Teo, W.E.; He, W.; Ramakrishna, S. Electrospun scaffold tailored for tissue-specific extracellular matrix, *Biotechnol J* **2006**, 1, 918-929.

[3] Rho, K.S.; Jeong, L.; Lee, G.; Seo, B.M.; Park, Y.J.; Hong, S.D.; Roh, S.; Cho, J.J.; Park, W.H.; Min, B.M. Electrospinning of collagen nanofibers: effects on the behavior of normal human keratinocytes and early-stage wound healing, *Biomaterials* **2006**, 27, 1452-1461.

[4] Reneker, D.H.; Yarin, A.L. Electrospinning jets and polymer nanofibers, *Polymer* **2008**, 49, 2387-2425.

[5] Meechaisue, C.; Dubin, R.; Supaphol, P.; Hoven, V.P.; Kohn, J. Electrospun Mat of Tyrosine-Derived Polycarbonate Fibers for Potential Use as Tissue Scaffolding Material, *J Biomater Sci Polym Ed* **2006**, 17, 1039-1056.

[6] Sangsanoh, P.; Waleetorncheepsawat, S.; Suwantong, O.; Wutticharoenmongkol, P.; Weeranantanapan, O.; Chuenjitbuntaworn, B.; Cheepsunthorn, P.; Pavasant, P.; Supaphol, P. In Vitro Biocompatibility of Schwann Cells on Surfaces of Biocompatible Polymeric Electrospun Fibrous and Solution-Cast Film Scaffolds, *Biomacromolecules* **2007**, 8, 1587-1594.

[7] Wutticharoenmongkol, P.; Pavasant, P.; Supaphol, P. Osteoblastic Phenotype Expression of MC3T3-E1 Cultured on Electrospun Polycaprolactone Fiber Mats Filled with Hydroxyapatite Nanoparticles, *Biomacromolecules* **2007**, 8, 2602-261.

[8] Chen, G.; Ushida, T.; Tateishi, T. Scaffold Design for Tissue Engineering, *Macromol Biosci* **2002**, 2, 67-77.

[9] Coombes, A.G.A.; Verderiob, E.; Shawa, B.; Lib, X.; Griffinb, M.; Downes, S. Biocomposites of non-crosslinked natural and synthetic polymers, *Biomaterials* **2002**, 23, 2113-2118.

[10] Masuko, T.; Iwasaki, N.; Yamane, S.; Funakoshi, T.; Majima, T.; Minami, A.; Ohsuga, N.; Ohta, T.; Nishimura, S.I. Chitosan-RGDSGGC conjugate as a scaffold material for musculoskeletal tissue engineering, *Biomaterials* **2005**, 26, 5339-5347.

[11] Boccafoschi, F.; Habermehl, J.; Vesentini, S.; Mantovani, D. Biological performances of collagen-based scaffolds for vascular tissue engineering, *Biomaterials* **2005**, 26, 7410-7417.

[12] Neamnark, A.; Sanchavanakit, N.; Pavasant, P.; Bunaprasert, T.; Supaphol, P.; Rujiravanit, R. In Vitro Biocompatibility Evaluations of Hexanoyl Chitosan Film, *Carbohyd Polym* **2007**, 68, 166-172.

[13] Ravi Kumar, M. A review of chitin and chitosan applications, *React Funct Polym* **2000**, 46, 1-27.

[14] Ohkawa, K.; Cha, D.; Kim, H.; Nishida, A.; Yamamoto, H. Electrospinning of Chitosan. *Macromol Rapid Comm* **2004**, 25, 1600-1605.

[15] Spasova, M.; Manolova, N.; Paneva, D.; Rashkov, L. Preparation of Chitosan Containing Nanofibers by Electrospinning Chitosan/Poly(ethylene oxide) Mixed Solutions, *e-Polymers* **2004**, No. 056, 1-12.

[16] Duan, B.; Dong, C.; Yuan, X.; Yao, K. Electrospinning of Chitosan Solutions in Acetic Acid with Poly(ethylene oxide), *J Biomater Sci Polym Ed* **2004**, 15, 797-811.

[17] Bhattarai, N.; Edmondson, D.; Veiseh, O.; Matsen, F.A.; Zhang, M. Electrospun chitosan-based nanofibers and their cellular compatibility, *Biomaterials* **2005**, 26, 6176-6184.

[18] Desai, K.; Kit, K.; Li, J.; Zivanovic, S. Morphological and Surface Properties of Electrospun Chitosan Nanofibers, *Biomacromolecules* **2008**, 9, 1000-1006.

[19] Zhang, Y.Z.; Su, B.; Ramakrishna, S.; Lim, C.T. Chitosan Nanofibers from an Easily Electrospinnable UHMWPEO-Doped Chitosan Solution System, *Biomacromolecules* **2008**, 9, 136-141.

[20] Park, W.H.; Jeong, L.; Yoo, D.I.; Hudson, S. Effect of Chitosan on Morphology and Conformation of Silk Fibroin Nanofibers, *Polymer* **2004**, 45, 7151-7157.

[21] Li, L.; Hsieh, Y.L. Chitosan bicomponent nanofibers and nanoporous fibers, *Carbohyd Res* **2006**, 341, 374-381.

[22] Duan, B.; Yuan, X.; Zhu, Y.; Zhang, Y.; Li, X.; Zhang, Y.; Yao, K. A nanofibrous composite membrane of PLGA–chitosan/PVA prepared by electrospinning, *Eur Polym J* **2006**, 42, 2013-2022.

[23] Zhang, Y.; Huang, X.; Duan, B.; Wu, L.; Li, S.; Yuan, X. Preparation of electrospun chitosan/poly(vinyl alcohol) membranes, *Colloid Polym Sci* **2007**, 285, 855-863.

[24] Jia, Y.T.; Gong, J.; Gu, X.H.; Kim, H.Y.; Dong, J.; Shen, X.Y. Fabrication and characterization of poly (vinyl alcohol)/chitosan blend nanofibers produced by electrospinning method, *Carbohyd Polym* **2007**, 67, 403-409.

[25] Huang, X.J.; Ge, D.; Xu, Z.K. Preparation and characterization of stable chitosan nanofibrous membrane for lipase immobilization, *Eur Polym J* **2007**, 43, 3710-3718.

[26] Sajeev, U.S.; Anand, K.A.; Menon, D.; Nair S. Control of nanostructures in PVA, PVA/chitosan blends and PCL through electrospinning, *Bulletin in Materials Science* **2008**, 31, 343-351.

[27] Zhou, Y.S.; Yang, D.Z.; Nie, J. Electrospinning of Chitosan/Poly(vinyl alcohol)/Acrylic Acid Aqueous Solutions, *J Appl Polym Sci* **2006**, 102, 5692-5697.

[28] Zhou, Y.S.; Yang, D.Z.; Nie, J. Preparation and characterization of crosslinked chitosan-based nanofibers, *Chinese Chem Lett* **2007**, 18, 118-120.

[29] Yang, D.; Jin, Y.; Zhou, Y.; Ma, G.; Chen, X.; Lu, F.; Nie, J. In Situ Mineralization of Hydroxyapatite on Electrospun Chitosan-Based Nanofibrous Scaffolds, *Macromol Biosci* **2008**, 8, 239-246.

[30] Ma, G.; Yang, D.; Zhou, Y.; Jin, Y.; Nie, J. Preparation and characterization of chitosan/poly(vinyl alcohol)/poly(vinyl pyrrolidone) electrospun fibers, *Front Mater Sci Chin* **2007**, 1, 432-436.

[31] Jung, K.H.; Huh, M.W.; Meng, W.; Yuan, J.; Hyun, S.H.; Bae, J.S.; Hudson, S.M.; Kang, I.K. Preparation and antibacterial activity of PET/chitosan nanofibrous mats using an electrospinning Technique, *J Appl Polym Sci* **2007**, 105, 2816-2823.

[32] Mo, X.; Chen, Z.; Weber, H.J. Electrospun nanofibers of collagen-chitosan and P(LLA-CL) for tissue engineering, *Front Mater Sci Chin* **2007**, 1, 20-23.

[33] Chen, Z.; Mo, X.; Qing, F. Electrospinning of collagen–chitosan complex, *Mater Lett* **2007**, 61, 3490-3494.

[34] Chen, Z.; Mo, X.; He, C.; Wang, H. Intermolecular interactions in electrospun collagen–chitosan complex nanofibers, *Carbohyd Polym* **2008**, 72, 410-418.

[35] Chen, J.P.; Chang, G.Y.; Chen, J.K. Electrospun collagen/chitosan nanofibrous membrane as wound dressing, *Colloids Surf A* **2008**, 313-314, 183-188.

[36] Desai, K.; Kit, K. Effect of spinning temperature and blend ratios on electrospun chitosan/poly(acrylamide) blends fibers, *Polymer* **2008**, 49, 4046-4050.

[37] Xu, J.; Zhang, J.; Gao, W.; Liang, H.; Wang, H.; Li, J. Preparation of chitosan/PLA blend micro/nanofibers by electrospinning, *Mater Lett* **2009**, 63, 658-660.

[38] Shalumon, K.T.; Binulal, N.S.; Selvamurugan, N.; Nair, S.V.; Deepthy, M.; Furuike, T.; Tamura, H.; Jayakumar, R. Electrospinning of carboxymethyl chitin/poly(vinyl alcohol) nanofibrous scaffolds for tissue engineering applications, *Carbohyd Polym* **2009**, 77, 863-869.

[39] Zhou, Y.; Yang, D.; Chen, X.; Xu, Q.; Lu, F.; Nie, J. Electrospun Water-Soluble Carboxyethyl Chitosan/Poly(vinyl alcohol) Nanofibrous Membrane as Potential Wound Dressing for Skin Regeneration, *Biomacromolecules* **2008**, 9, 349–354.

[40] Neamnark, A.; Rujiravanit, R.; Supaphol, P. Electrospinning of hexanoyl chitosan, *Carbohyd Polym* **2006**, 66, 298–305.

[41] Ignatova, M.; Manolova, N.; Rashkov, I. Novel antibacterial fibers of quaternized chitosan and poly(vinyl pyrrolidone) prepared by electrospinning, *Eur Polym J* **2007**, 43, 1112–1122.

[42] Ignatova, M.; Starbova, K.; Markova, N.; Manolova, N.; Rashkov, I. Electrospun nano-fibre mats with antibacterial properties from quaternised chitosan and poly(vinyl alcohol), *Carbohyd Res* **2006**, 341, 2098–2107.

[43] Sangsanoh, P.; Supaphol, P. Stability Improvement of Electrospun Chitosan Nanofibrous Membranes in Neutral or Weak Basic Aqueous Solutions, *Biomacromolecules* **2006**, 7, 2710-2714.

[44] Ohkawa, K.; Minato, K.; Kumagai, G.; Hayashi, S.; Yamamoto, H. Chitosan Nanofiber, *Biomacromolecules* **2006**, 7, 3291-3294.

[45] Duan, B.; Wu, L.; Yuan, X.; Hu, Z.; Li, X.; Zhang, Y.; Yao, K.; Wang, M. Hybrid nanofibrous membranes of PLGA/chitosan fabricated via an electrospinning array, *J Biomed Mater Res* **2007**, 83A, 868-878.

[46] Schiffman, J.D.; Schauer, C.L. Cross-Linking Chitosan Nanofibers, *Biomacromolecules* **2007**, 8, 594-601.

[47] Schiffman, J.D.; Schauer, C.L. One-Step Electrospinning of Cross-Linked Chitosan Fibers, *Biomacromolecules* **2007**, 8, 2665-2667.

[48] Torres-Giner, S.; Ocio, M.J.; Lagaron, J.M. Development of Active Antimicrobial Fiber Based Chitosan Polysaccharide Nanostructures using Electrospinning, *Engineering in Life Science* **2008**, 3, 303-314.

[49] Wan, Y.; Cao, X.; Zhang, S.; Wang, S.; Wu, Q. Fibrous poly(chitosan-g-DL-lactic acid) scaffolds prepared via electro-wet-spinning, *Acta Biomater* **2008**, 4, 876-886.

[50] Prabhakaran, M.P.; Venugopal, J.; Chyan, T.T.; Hai, L.B.; Chan, C.K.; Tang, A.L.Y.; Ramakrishna, S. Electrospun Biocomposite Nanofibrous Scaffolds for Neural Tissue Engineering, *Tissue Eng A* **2008**, 14, 1781-1791.

[51] Wang, W.; Itoh, S.; Konno, K.; Kikkawa, T.; Ichinose, S.; Sakai, K.; Ohkuma, T.; Watabe, K. Effects of Schwann cell alignment along the oriented electrospun chitosan nanofibers on nerve regeneration, *J Biomed Mater Res* **2008**, DOI: 10.1002/jbm.a.32329.

[52] Min, B.M..; Lee, S.W.; Lim, J.N.; You, Y.; Lee, T.S.; Kang, P.H.; Park, W.H. Chitin and chitosan nanofibers: electrospinning of chitin and deacetylation of chitin nanofibers, *Polymer* **2004**, 45, 7137-7142.

[53] Geng, X.; Kwon, O.H.; Jang, J. Electrospinning of chitosan dissolved in concentrated acetic acid solution, *Biomaterials* **2005**, 26, 5427-5432.

[54] De Vrieze, S.; Westbroek, P.; van Camp, T.; van Langenhove, L. Electrospinning of chitosan nanofibrous structures: feasibility study, *J Mater Sci* **2007**, 42, 8029-8034.

[55] Ojha, S.S.; Stevens, D.R.; Hoffman, T.J.; Stano, K.; Klossner, R.; Scott, M.C.; Krause, W.; Clarke, L.I.; Gorga, R.E. Fabrication and Characterization of Electrospun Chitosan Nanofibers Formed via Templating with Polyethylene Oxide, *Biomacromolecules* **2008**, 9, 2523-2529.

[56] Mano, J.F.; Silva, G.A.; Azevedo, H.S.; Malafaya, P.B.; Sousa, R.A.; Silva, S.S.; Boesel, L.F.; Oliveira, J.M.; Santos, T.C.; Marques, A.P.; Neves, N.M.; Reis, R.L. Natural origin biodegradable systems in tissue engineering and regenerative medicine: present status and some moving trends, *J R Soc Interface* **2007**, 4, 999-1030.

[57] Bunge, R.P. The role of the Schwann cell in trophic support and regeneration, *J Neurol* **1994**, 241, S19-S21.

[58] Yuan, Y.; Zhang, P.; Yang, Y.; Wang, X.; Gu, X. The interaction of Schwann cells with chitosan membranes and fibers in vitro, *Biomaterials* **2004**, 25, 4273-4278.

[59] Wenling, C.; Duohui, J.; Jiamou, L.; Yandao, G.; Nanming, Z.; Zhang, X. Effects of the Degree of Deacetylation on the Physicochemical Properties and Schwann Cell Affinity of Chitosan Films, *J Biomater Appl* **2005**, 20, 157-177

[60] Fakhry, A.; Schneider, G.B.; Zaharias, Ş.S. Chitosan supports the initial attachment and spreading of osteoblasts preferentially over fibroblasts, *Biomaterials* **2004**, 25, 2075-2079.

[61] Spasavo. M.; Paneva, D.; Manolova, N.; Radenkov, P.; Rashkov, I. Electrospun Chitosan-Coated Fibers of Poly(L-lactide) and Poly(L-lactide)/Poly(ethylene glycol): Preparation and Characterization, *Macromol Biosci* **2008**, 8, 153-162.

[62] Prasitsilp, M.; Jenwithisuk, R.; Kongsuwan, K.; Damrongchai, N.; Watts, P. Cellular responses to chitosan in vitro: the importance of deacetylation, *J Mater Sci - Mater Med* **2000**, 11, 773-778.

[63] Chatelet, C.; Damour, O.; Domard, A. Influence of the degree of acetylation on some biological properties of chitosan films, *Biomaterials* **2001**, 22, 261-268.

[64] Howling, G.I.; Dettmar, P.W.; Goddard, P.A.; Hampson, F.C.; Dornish, M.; Wood, E.J. The effect of chitin and chitosan on the proliferation of human skin fibroblasts and keratinocytes in vitro, *Biomaterials* **2001**, 22, 2959-2966.

[65] Hamilton, V.; Yuan, Y.; Rigney, D.A.; Puckett, A.D.; Ong, J.L.; Yang, Y.; Elder, S.H.; Bumgardner, J.D. Characterization of chitosan films and effects on fibroblast cell attachment and proliferation, *J Mater Sci - Mater Med* **2006**, 17, 1373-1381.

[66] Minagawa, T.; Okamura, Y.; Shigemasa, Y.; Minami, S.; Okamoto, Y. Effects of molecular weight and deacetylation degree of chitin/chitosan on wound healing, *Carbohyd Polym* **2007**, 67, 640-644.

[67] Johnen, C.; Steffen, I.; Beichelt, D.; Bräutigam, K.; Witascheck, T.; Toman, N.; Moser, V.; Ottomann, C.; Hartmann, B.; Gerlach, J.C. Culture of subconfluent human fibroblasts and keratinocytes using biodegradable transfer membranes, *Burn* **2008**, 34, 655-663.

[68] Burns, N.L.; Holmberg, K.; Brink, C. Influence of surface charge on protein adsorption at an amphoteric surface: effects of varying acid to base Ratio, *J Colloid Interf Sci* **1996**, 178, 116–122.

[69] Webb, K.; Hlady, V.; Tresco, P.A. Relative importance of surface wettability and charged functional groups on NIH 3T3 fibroblast attachment, spreading, and cytoskeletal organization, *J Biomed Mater Res* **1998**, 41, 422–430.

[70] Knopf, B.; Wollina, U. Electrophoretic mobilities of keratinocytes from normal skin and psoriatic lesions, *Arch Dermatol Res* **1992**, 284, 117-118.

[71] Anthonsen, W.M.; Varum, K.M.; Smidsrod, O. Solution properties of chitosans: conformation and chain stiffness of chitosans with different degrees of N-acetylation, *Carbohydr Polym* **1993**, 22, 193–201.

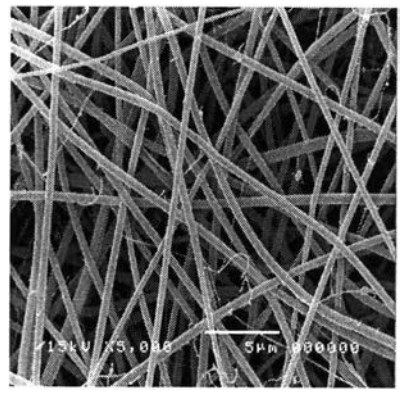

Figure 3.1 Selected SEM images of free-standing chitosan nanofibers before cell culture.

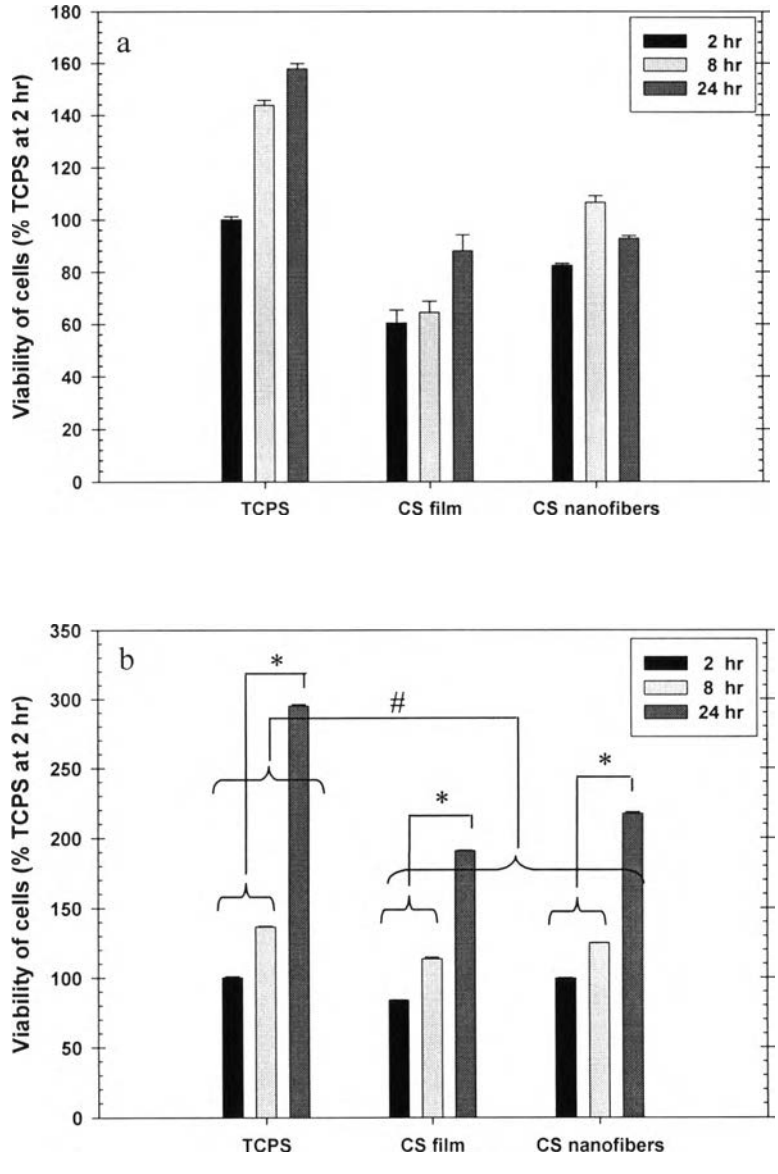

Figure 3.2 Attachment of (a) murine Schwann cells (RT4-D6P2T), (b) murine osteoblast-like cells (MC3T3-E1), (c) human keratinocytes (HaCaT), and (d) human fibroblasts (HFF) that had been seeded on electrospun chitosan nanofibers and corresponding solution-cast film substrates and TCPS (i.e., control) for 2, 8 and 24 h. The viability of the attached cells that had been seeded on TCPS for 2 h was used as reference to calculate the relative viability of the attached cells shown in the figure. *, # are significantly different at $p < 0.05$.

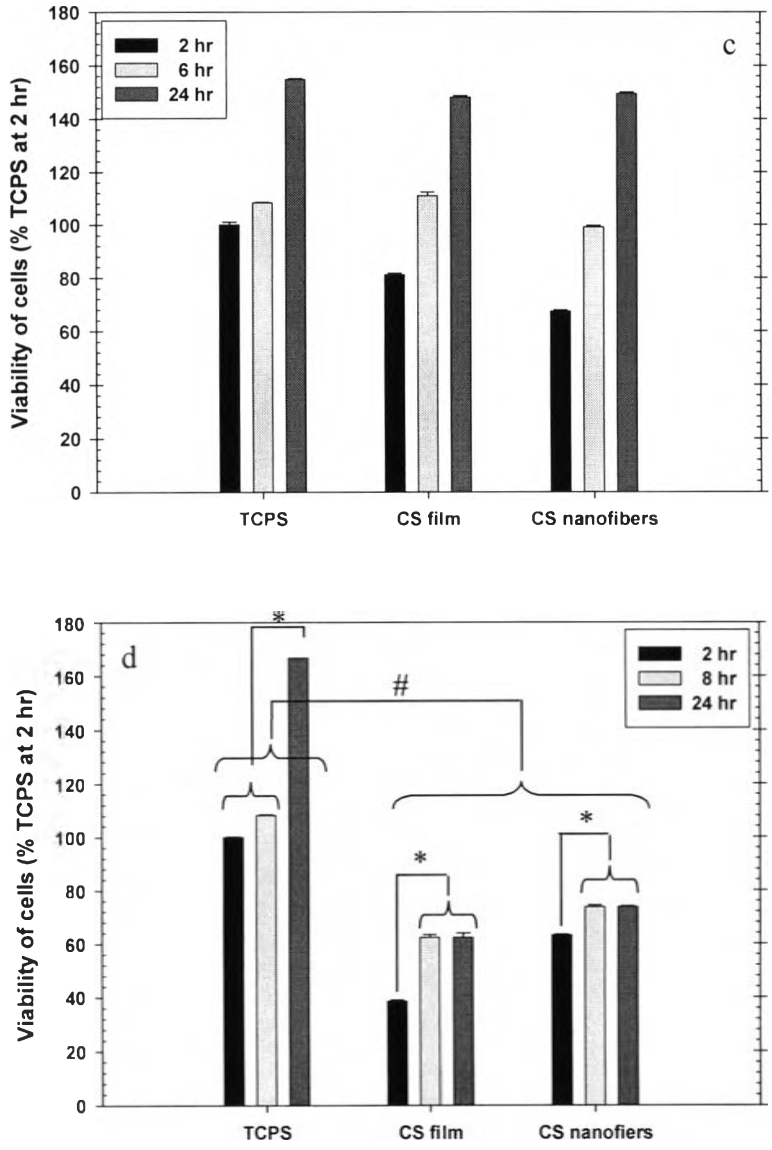

Figure 3.2 (cont.)

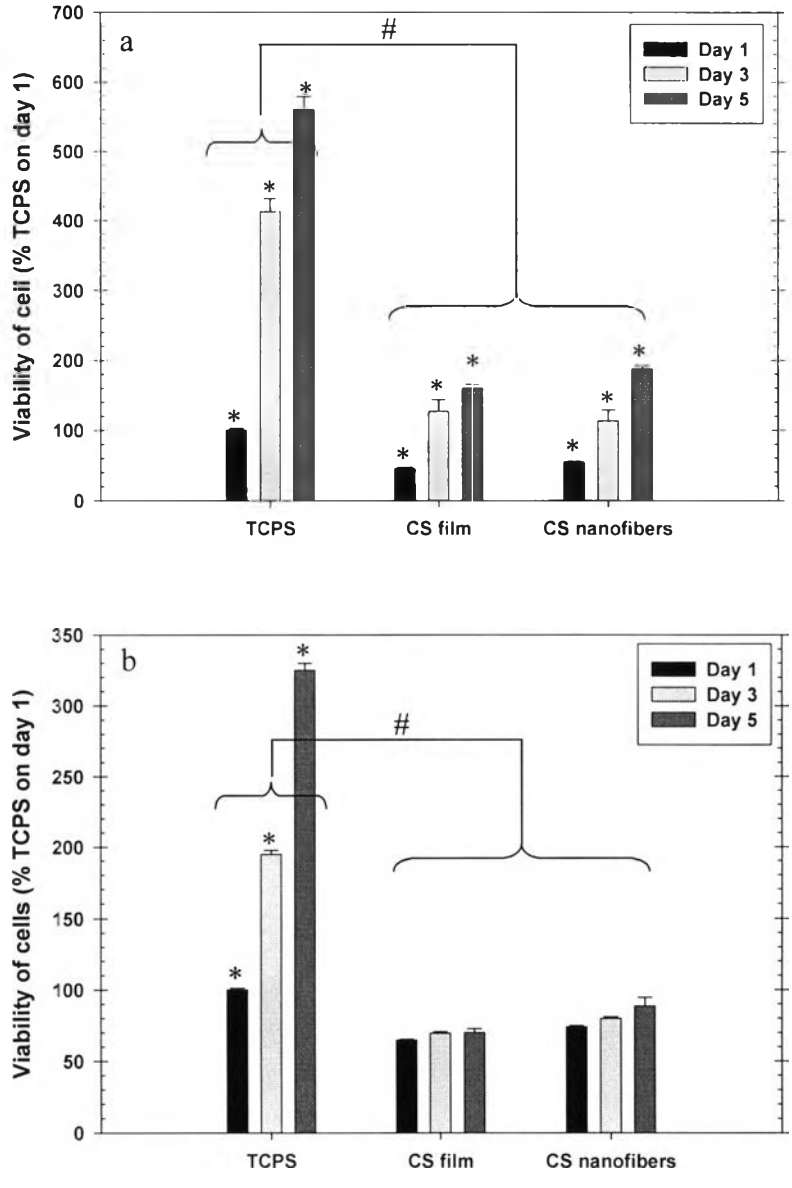

Figure 3.3 Proliferation of (a) murine Schwann cells (RT4-D6P2T), (b) murine osteoblast-like cells (MC3T3-E1), (c) human keratinocytes (HaCaT), and (d) human fibroblasts (HFF) that had been cultured on electrospun chitosan nanofibers and corresponding solution-cast film substrates and TCPS (i.e., control) for 1, 3 and 5 d. The viability of the attached cells that had been cultured on TCPS for 1 d was used as reference to calculate the relative viability of the proliferated cells shown in the figure. *, # are significantly different at $p < 0.05$.

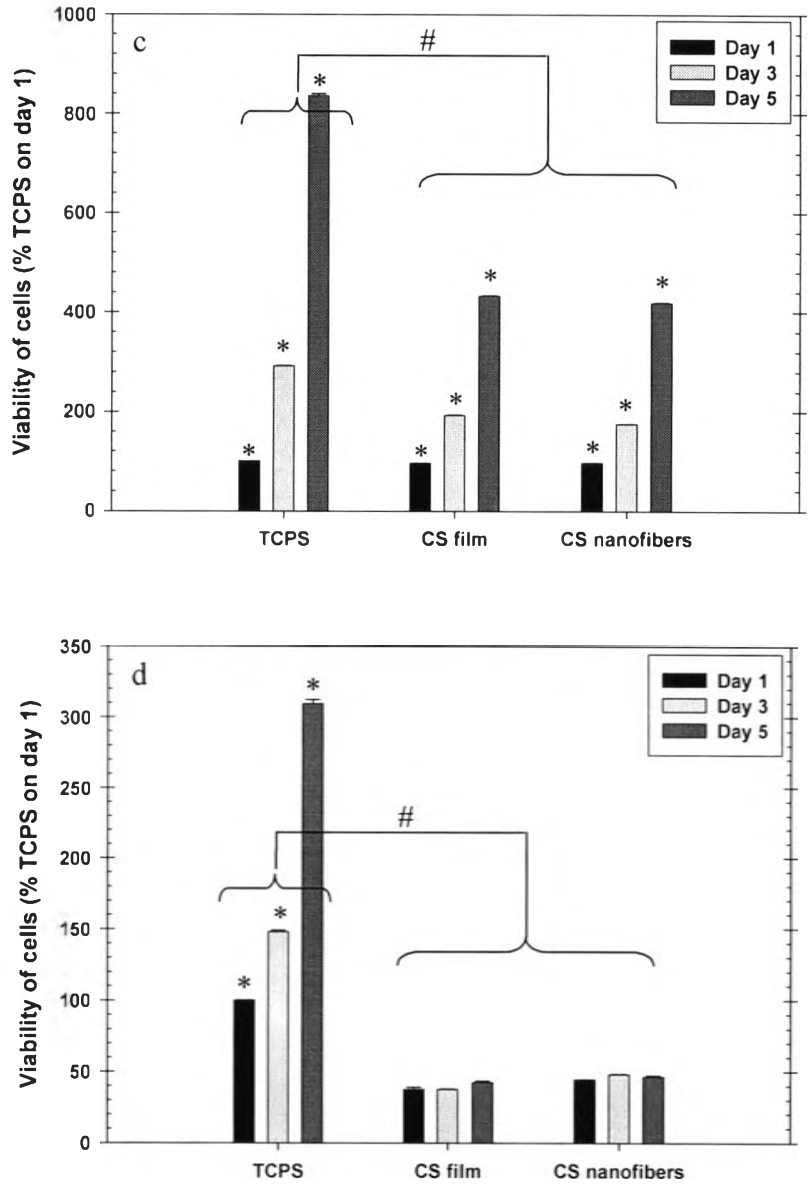

Figure 3.3 (cont.)

Table 3.1 Representative SEM images of murine Schwann cells (RT4-D6P2T) hat had been seeded or cultured on electrospun chitosan (CS) nanofibers and corresponding solution-cast film substrates and TCPS (i.e., control) for 2 h, 8 h, 1 d, 3 d and 5 d.

Cell seeding/culturing time point	Type of substrate		
	Glass	CS nanofiber	CS film
2 h		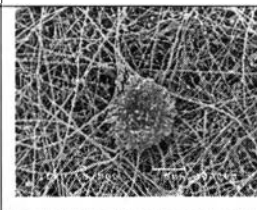	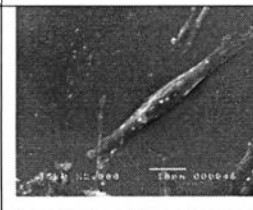
8 h	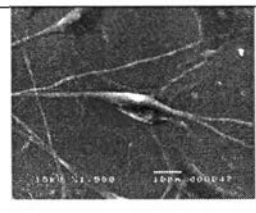	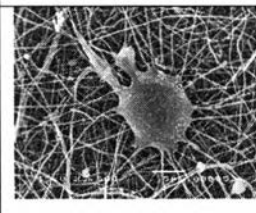	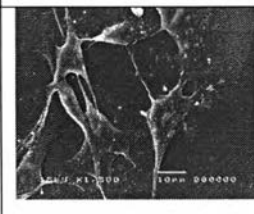
24 h or 1 d	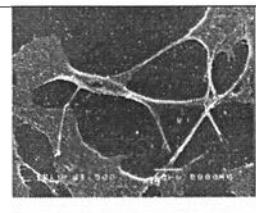	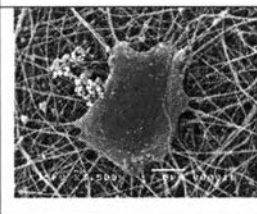	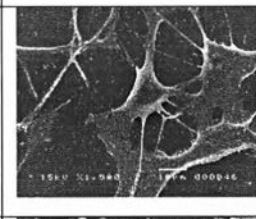
3 d		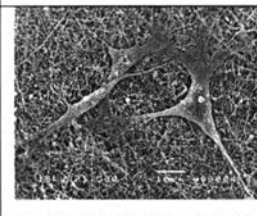	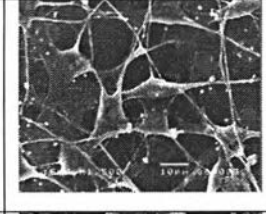
5 d	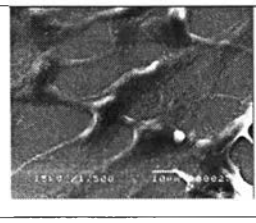		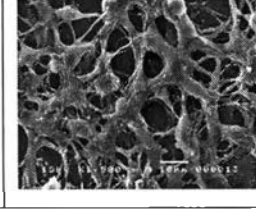

Table 3.2 Representative SEM images of murine osteoblast-like cells (MC3T3-E1) that had been seeded or cultured on electrospun chitosan (CS) nanofibers and corresponding solution-cast film substrates and TCPS (i.e., control) for 2 h, 8 h, 1 d, 3 d and 5 d.

Cell seeding/culturing time point	Type of substrate		
	Glass	CS nanofibers	CS film
2 h	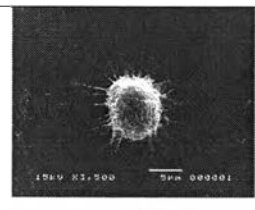	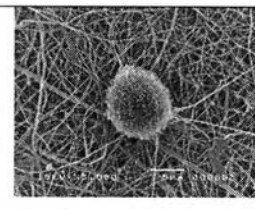	
8 h	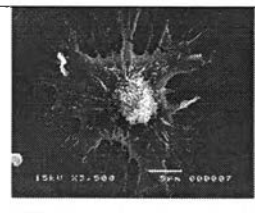	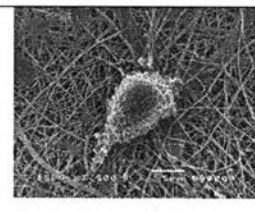	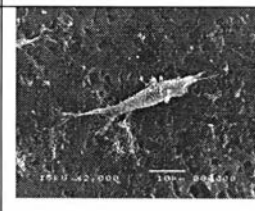
24 h or 1 d	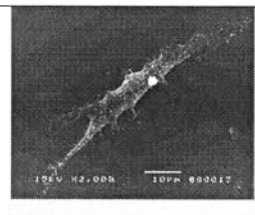	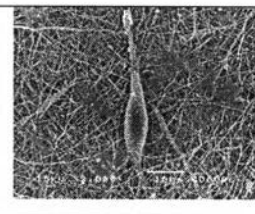	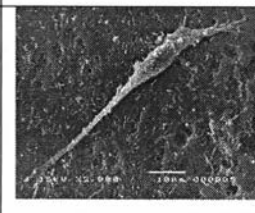
3 d		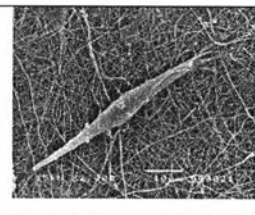	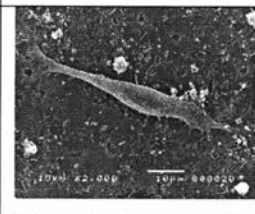
5 d	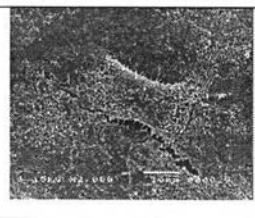	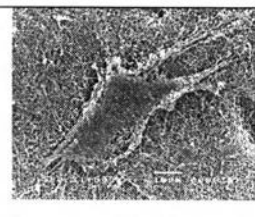	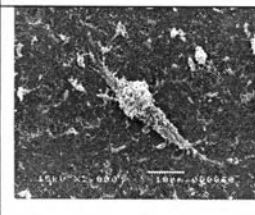

Table 3.3 Representative SEM images of human keratinocytes (HaCaT) hat had been seeded or cultured on electrospun chitosan (CS) nanofibers and corresponding solution-cast film substrates and TCPS (i.e., control) for 2 h, 8 h, 1 d, 3 d and 5 d.

Cell seeding/culturing time point	Type of substrate		
	Glass	CS nanofibers	CS film
2 h	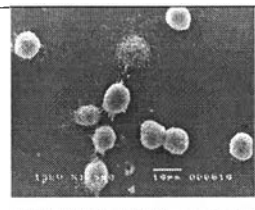	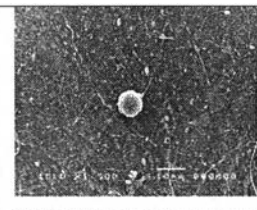	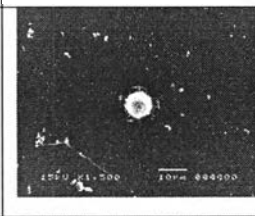
8 h	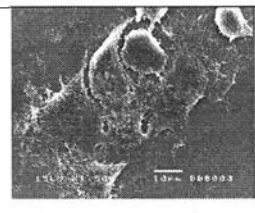	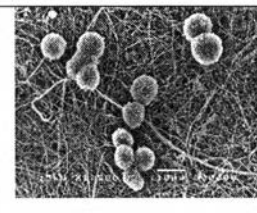	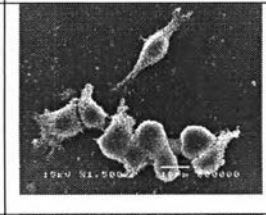
24 h or 1 d	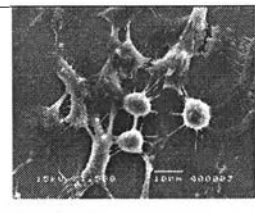	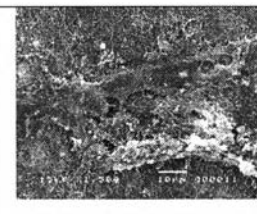	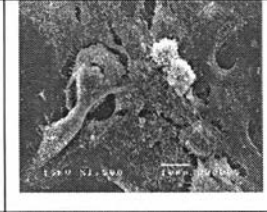
3 d	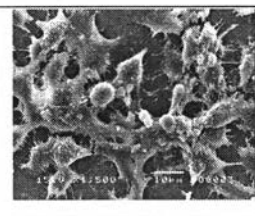	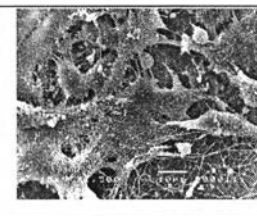	
5 d	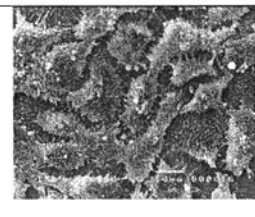	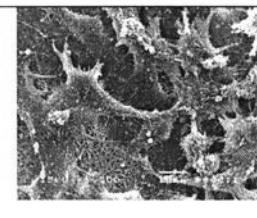	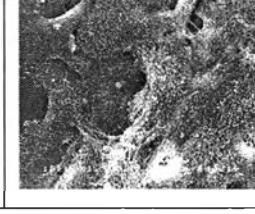

Table 3.4 Representative SEM images of human fibroblasts (HFF) hat had been seeded or cultured on electrospun chitosan (CS) nanofibers and corresponding solution-cast film substrates and TCPS (i.e., control) for 2 h, 8 h, 1 d, 3 d and 5 d.

Cell seeding/culturing time point	Type of substrate		
	Glass	CS nanofibers	CS film
2 h	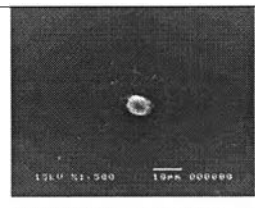	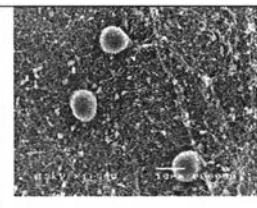	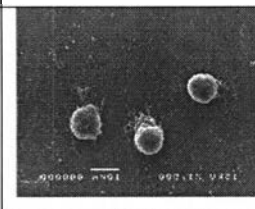
8 h	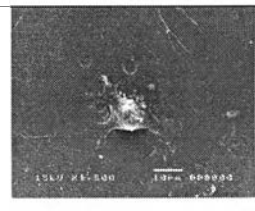	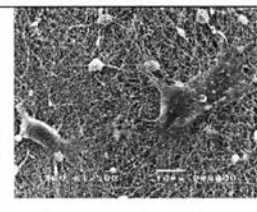	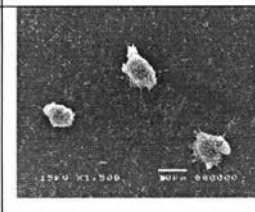
24 h or 1 d	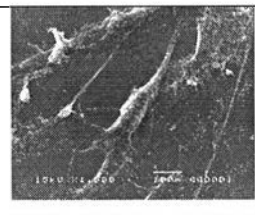		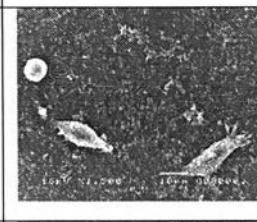
3 d	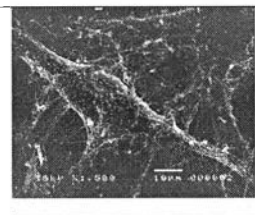	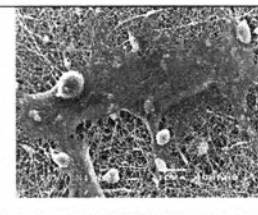	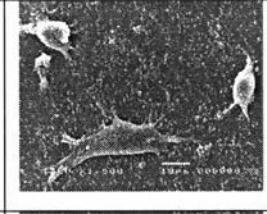
5 d	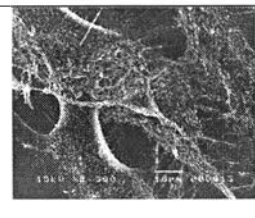	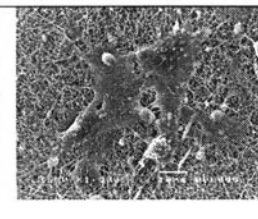	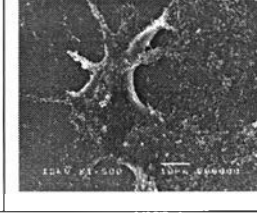

Supporting Information

Characterization of Chitosan

Degree of Deacetylation (%DDA)

In order to determine the degree of deacetylation (%DDA) of chitosan, ^{1}H-NMR spectroscopy (VARIAN UNITY INOVA 500 MHz NMR) was used. The measurements were performed by dissolving ~ 5 mg of the as-received chitosan powder in 2 wt.% CD_3COOD/D_2O at 24 °C. The %DDA value is evaluated by the method utilized by Hirai et al. [Hirai, A.; Odani, H.; Nakajima, A. *Polymer Bulletin* **1991**, *26*, 87], which bases their calculation on the ratio between the integral intensity of CH_3 residue (I_{CH_3}) and the summation of the integral intensities of protons at 2, 3, 4, 5, 6 and 6' positions ($I_{H2\text{-}H6}$), that is

$$\%DDA = 1-\left(\frac{1}{3}I_{CH_3} / \frac{1}{6}I_{H2\text{-}H6}\right) \qquad (1s)$$

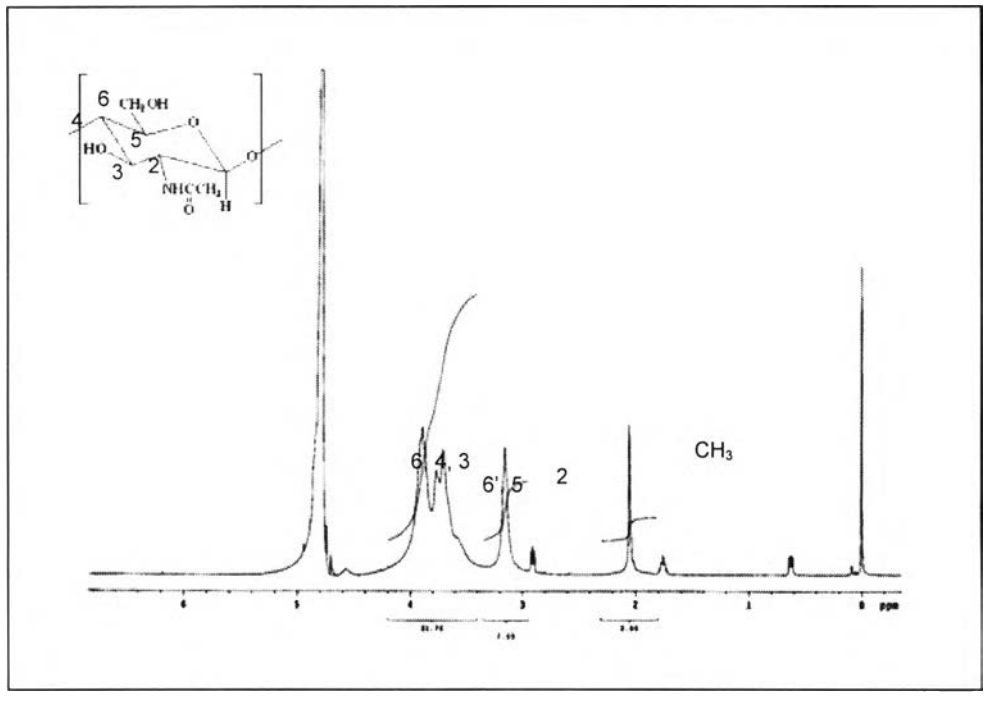

Figure 3.1s ^{1}H-NMR spectrum of chitosan in 2 wt.% CD_3COOD/D_2O.

Table 3.1s ^{1}H-NMR integral intensities for chitosan in 2 wt.% CD_3COOD/D_2O.

Protons	Chemical shift (ppm)	Integral intensity
N-acetyl	2.054	3.00
H2	3.154	7.69
H3, 4, 5, 6, 6'	3.908, 3.888, 3.866, 3.766, 3.704	31.76

Molecular Weight Determination

Both the weight-average and the number-average molecular weights of chitosan were determined using a Waters 600E gel permeation chromatograph [eluent = 0.5 M acetic acid and 0.5 M sodium acetate (i.e., acetate buffer, pH ~ 4); column = Ultrahydrogel linear (Mw resolving range = 1,000-20,000,000 g/mol); polymer standard = polysaccharide (Pullulans: Mw 5,900-788,000 g/mol); calibration method = polysaccharide standard calibration; detector = refractive index; temperature = 30 °C; software = PL LogiCal].

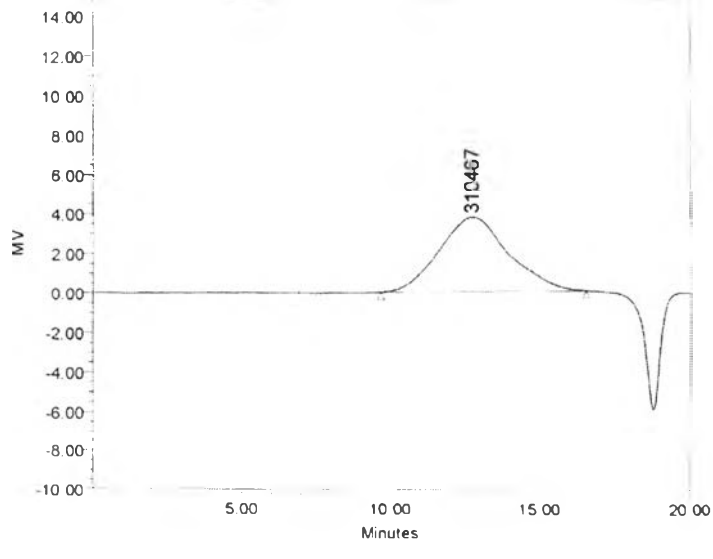

Figure 3.2s Molecular weight distribution of chitosan.

Table 3.2s Molecular weight distribution of chitosan by gel permeation chromatography technique.

Sample	M_n (kg/mol)	M_w (kg/mol)	M_v (kg/mol)	Polydispersity
Chitosan	110	610	310	5.8

Additional Experiments

Effect of Concentration of Chitosan Solutions on Morphology of Electrospun Fibers

Experimental. To further demonstrate the effect of concentration of the chitosan solution in TFA/DCM on the morphology of the electrospun chitosan nanofibrous membranes, 5-8% w/v chitosan solutions were prepared by dissolving a measured amount of chitosan powder in 70:30 v/v TFA/DCM mixture. The as-prepared chitosan solutions were stirred continuously for 12 h at room temperature and later fed into a 5-mL glass syringe fitted with a blunt 20-gauge stainless steel needle (OD = 0.91 mm), used as the nozzle. Both the syringe and the needle were tilted 45° from a horizontal baseline. The distance from the needle tip to the screen was fixed at 20 cm. The needle was connected to the emitting electrode of positive polarity of a Gamma High-Voltage Research ES30P-5W power supply. Both the electrical potential and the collection time were fixed at 25 kV and 5 min. The solution feed rate was driven mainly by the gravity and the electrostatic forces generated during e-spinning. The resulting chitosan nanofibrous membranes were dried *in vacuo* at room temperature prior to observation in SEM.

Results. According to the results shown in Figure 3s, a combination of smooth and beaded fibers was obtained from 5 and 6% w/v chitosan solutions. The size of these fibers was rather irregular. At 7 and 8% w/v, predominantly smooth fibers were obtained. The size of these fiber was more uniform.

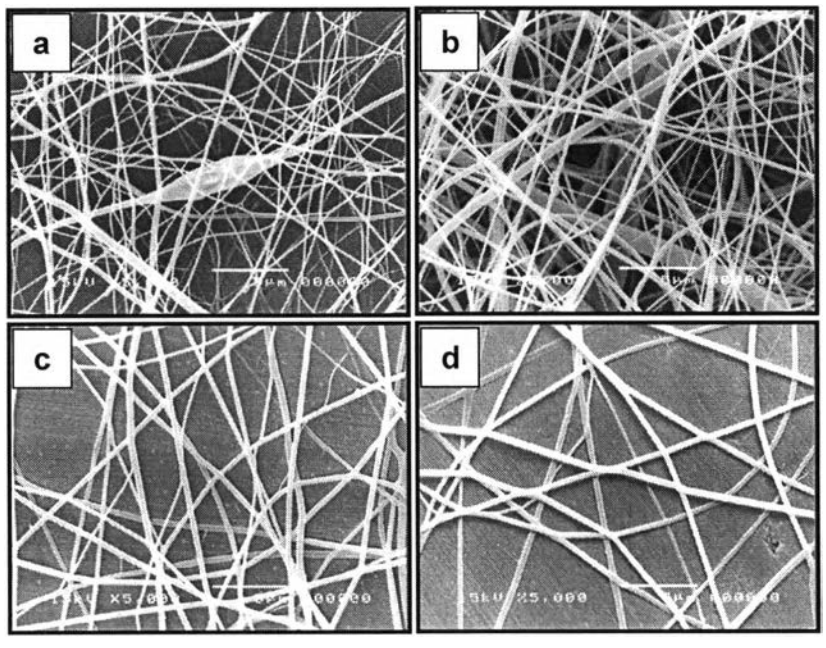

Figure 3.3s Selected SEM images of electrospun chitosan nanofibers at (a) 5, (b) 6, (c) 7 and (d) 8% w/v chitosan solutions by dissolving a measured amount of chitosan powder in 70:30 v/v TFA/DCM mixture and stirred continuously for 12 h at room temperature. The distance from the needle tip to the screen was fixed at 20 cm. The electrical potential and the collection time were 25 kV and 5 min.

Morphology of Solvent-Cast Chitosan Films

Experimental. To illustrate the effect of the casting solvent on morphology of the obtained chitosan films, two types of the solvent system were studied: 1 wt.% acetic acid aqueous solution (as used in the present work) and 70:30 v/v trifluoroacetic acid (TFA)/dichloromethane (DCM) mixture (as used in the preparation of the electrospun chitosan fibers in this work).

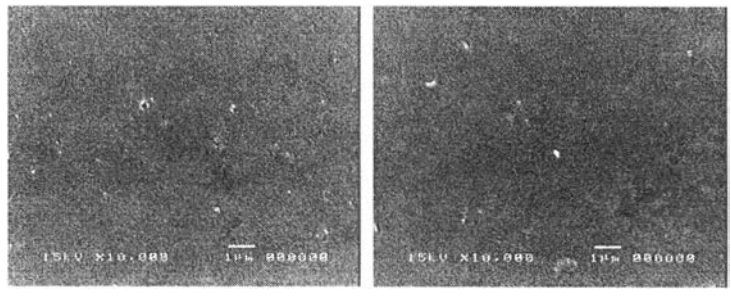

Figure 3.4s Representative SEM images illustrating the surface morphology of chitosan films that had been casted from 2.5% w/v chitosan solutions in (left) 1 wt.% acetic aqueous solution and (right) 70:30 v/v TFA/DCM.

Results. It is clear that the choice of solvent system used to fabricate chitosan films had no profound effect on the surface topography of the obtained films.